

# TEC Forecasting using Optimized Variational Mode Decomposition and Elman Neural Networks

Maladh Mahmood Shakir, Zalinda Othman, Azuraliza Abu Bakar  
Faculty of Information Science and Technology  
University Kebangsaan Malaysia  
Bangi, Selangor, Malaysia

**Abstract**—Forecasting the ionosphere layer's total electronic content (TEC) is crucial for its impact on satellite signals and global positioning systems (GPS) and the ability to predict earthquakes. The existing statistical-based forecasting models such as ARMA, ARIMA, and HW suffered from the TEC non-stationarity nature, which requires algorithmic handling of the forecasting and the mathematical part. This study proposes a hybrid method that incorporates several components and is designated as Optimized Variational Mode Decomposition with Recursive Neural Network Forecasting (OVMD-RNN) to forecast TEC. Before using the Elman Network to train each component, Variational Mode Decomposition (VMD) was used to decompose the signal into its essential stationary components. In addition, the proposed method includes an optimization algorithm for determining the best VMD decomposer parameters. The GPS Ionospheric Scintillation and TEC Monitor (GISTM) at Universiti Kebangsaan Malaysia station have been used to evaluate the method based on collected datasets for three years, 2011, 2012, and 2013. The experiment findings show that the model has successfully tracked all the up and down patterns in the time series. The results also reveal that VMD-based training might not always provide good results due to the residual signal. Finally, the evaluation focused on generating loss value and comparing it to the ARIMA benchmark. It showed that OVMD-RNN had accomplished a maximum improvement percentage of ARIMA with a value of (99%).

**Keywords**—Elman neural networks; forecast; hybrid model; optimized Variational Mode Decomposition; total electronic content

## I. INTRODUCTION

The global navigation satellite system (GNSS) has become a critical system for providing a wide range of services and applications in the modern world. As a result, its dependability and performance are critical for various systems. The state of the ionosphere and its amount of influence by solar radiation and the geomagnetic field is one of the factors that affect GNSS radio communication transmissions [1].

Researchers utilise a quantitative metric to explain the effect of solar radiation on the total electron content (TEC) of the ionosphere layer. This variable represents the variability of solar radiation's impacts on the ionosphere layer, as well as its geographically and temporally represented global positioning system (GPS) coordinates and time information. A dependable and accurate TEC forecasting can provide useful feedback to GPS receivers and improve numerous GPS-dependent services. Scientists created the International Reference Ionosphere (IRI) project to anticipate electron density, ion

composition, electron and ion temperature, and vertical electron column density due to the relevance of ionosphere prediction. As a result, IRI is a collaborative international initiative of the Committee on Space Research (COSPAR) and the International Union of Radio-science (URSI) to build and refine a reference model for the Earth ionosphere's most critical plasma properties [2].

The main goal of majoring in TEC is to foresee any delays in GPS or communication signals in general, which could impair the operation of numerous devices. Earthquake forecasting is another application of measuring and evaluating TEC. Studies have shown that the ionosphere is influenced by the Sun's position and radiation and geomagnetic activity, and seismic activity in the Earth's crust and surface. These impacts can aid in predicting an earthquake several days ahead of time [3].

The challenging aspect of TEC prediction is its non-stationarity nature. This has brought a limitation to the existing studies that uses statistical-based forecasting models such as ARMA, ARIMA, and HW [4]. Hence, researchers have tested the capability of neural networks in the general and recursive types of neural networks [5]. The latter is more preferred because of its feedback or memory aspect, which enables more flexibility in modelling the dynamics of the time series. However, RNN is not sufficient because of embedded non-stationarity in the time series, which requires algorithmic handling of the forecasting in addition to the mathematical part. VMD decomposition is a possible candidate for decomposing the original time series into various stationary components [6]. However, it is still encountering an issue in deciding the optimal number of intrinsic mode components for better forecasting performance and obtaining optimal VMD components before forecasting is needed. Hybrid architecture is a good candidate approach through combining RNN with optimal VMD settings. With such a hybrid combination, the VMD will decompose the original time series into stationary components that are easier to be learned by the following RNN layer.

The current forecasting models suffered from the TEC non-stationarity nature. This study describes a new method for forecasting the TEC time series that combines three components: decomposing the original signal to its stationary components using Variational Mode Decomposition (VMD), parameter optimization using Genetic Algorithm (GA), and forecasting using the Elman Neural Network, a well-known Recurrent Neural Network (Elman NN).

In the next Section II, related works on TEC forecasting and current approaches have been presented. In Section III, the proposed method has been described, i.e., OVMD-RNN and the methodology flow. The experimental works have been presented in Section IV as well as the results, whereas Section V gives conclusions.

## II. RELATED WORK

TEC forecasting increases the knowledge of ionosphere space weather to give accurate warning and mitigation of TEC impacts. Due to the time-series nature of TEC forecasting, researchers prefer traditional time series forecasting models such as Auto Regression Moving Average (ARMA) and its derivatives [7]. The VMD-ARMA (VARMA) model is described in [8] as a non-stationary signal decomposition technique based on Variational Mode Decomposition (VMD) paired with Auto Regressive Moving Average (ARMA) to estimate ionosphere delay values 1-hour ahead.

However, despite their large training requirements, some researchers have favoured non-linear models with a high approximation, such as Artificial Neural Networks (ANN) [9]. The TEC signal's non-linear nature is one of the factors driving the researchers' interest in employing ANN models for TEC forecasting. [10] is one of the first researchers to use ANN for TEC forecasting, further aided by [11]. According to them, the capacity to use ANN to predict TEC in places where appropriate training data was absent has been demonstrated empirically. [11] used ANN with a single hidden layer in addition to input and output layers, as described by the 6:9:1 configuration.

According to the newest research, a single hidden layer is sufficient, and adding more layers necessitates more training without increasing accuracy. However, studies have shown that ANN does not outperform basic linear models like ARMA and Auto Regressive Integrated Moving Average (ARIMA) [1], which is essentially ARMA plus an integration component. Both ARMA and ARIMA have outperformed the IRI global reference model. ARMA's and ARIMA's superiority Holt-Winter models, which add a component for seasonable effect, were also seen compared to the global IRI model [12, 13]. Several scholars have made a comparison of ARIMA with ANN. Based on mean absolute error (MAE) and root mean square error (RMSE) values, the performance of the ARMA and ANN models are validated on both geomagnetic quiet and disturbed days [14]. For the ARMA and ANN models, forecasting errors are higher on geomagnetically disturbed days; when tested using MAE and RMSE, ANN outperformed ARMA. Hybrid models of ARMA and ARIMA were used in other investigations. For 1-hour ahead forecast of ionosphere TEC, [12] used hybrid ARIMA models based on Wavelet Transform (WT) and Empirical Mode Decomposition (EMD).

A hybrid GA and ANN model was suggested by [15] to forecast 1-hour vertical TEC for one station in China. The Backpropagation Neural Network (BP) and the GA approach train parameters in a two-step process. GA tunes the weights and biases of the original neural network in the first stage. Model's weights and biases are recorded as a lengthy

chromosome. The fitness function expressed as a prediction error is used to evaluate each chromosome's performance in the population. A Wavelet Neural Network (WNN) is utilised to model the ionosphere time series in Iran by [16]. WNN is a hybrid of wavelet theory and neural network theory. One of the advantages of TEC modelling with WNN is its ease of use and speed of computation.

More recent studies have used machine learning algorithms for GPS TEC forecasting. The performance of a Gaussian kernel-based machine learning algorithm was compared to that of ANN and ARMA in [1]. The outcomes of their work have demonstrated dominance over them.

the authors in [17] employed a hybrid model in which the TEC time series was divided into its stationary components using VMD. Then a kernel extreme learning machine was used to anticipate the data. Kernel extreme learning machines were compared to ANN in this study, and the results show that the former is superior in forecasting accuracy. The idea of combining VMD with neural networks can be found in older time series forecasting research. Integration of VMD and generic regression neural networks is the focus of [17].

Another example is [18], who used VMD in conjunction with an extreme learning machine to model the Monthly Precipitation Time Series. Overall, researchers have attempted to forecast TEC time series in various locations for accomplishing needed actions such as handling delays of satellite signals GPS and forecasting earthquakes.

## III. PROPOSED METHOD

This study proposes a time series forecasting model using a VMD, and ENN hybrid architecture called an Optimized Variational Mode Decomposition with Elman Recursive Neural Network Forecasting (OVMD-RNN). It contains the following contributions.

- It develops a framework for TEC forecasting based on decomposition, optimization and ENN.
- It provides GA for finding the optimal IMF components  $K$  and the correlation coefficients  $\alpha$  for VMD.
- It integrates the developed OVMD by GA with ENN for forecasting the TEC.
- It evaluates the hybrid framework based on our data and compares it with recent models in the literature.

### A. Preliminary

1) *Variational mode decomposition*: The application of VMD is the initial step in the approach. The purpose of VMD is to decompose the TEC signal into bandwidth-limited components of varying frequencies. The decomposition helps eliminate the signal's random behavior and makes it more forecastable. Before VMD, researchers discovered various decomposition techniques, including Fourier transforms, wavelet transforms, and EMD [19]. However, research has shown that VMD outperforms EMD.

In the VMD algorithm [20], the real-valued input signal is viewed as an ensemble of sub-signals (modes) with a narrow band of frequencies around a few light frequencies. The VMD algorithm is represented as a variational problem with constraints:

$$\min_{\{u_k\}, \{\omega_k\}} \left\{ \sum_k \left\| \partial_t \left[ \left( \delta(t) + \frac{j}{\pi t} \right) * u_k(t) \right] e^{-j\omega_k t} \right\|_2^2 \right\} \quad (1)$$

s.t  $\sum_k u_k = f$

where,  $u_k$  denotes variational model components, and  $\omega_k$  are the corresponding centres of each variation model component.

The optimization is solved using Lagrangian multiplier  $\lambda$  and quadratic penalty  $\alpha$  as follows;

$$L(u_k, \omega_k, \lambda) = \alpha \sum_k \left\| \partial_t \left[ \left( \delta(t) + \frac{j}{\pi t} \right) * u_k(t) \right] * e^{-j\omega t} \right\|_2^2 + \|f - \sum_k u_k\|_2^2 + \langle \lambda, f - \sum_k u_k \rangle \quad (2)$$

The augmented Lagrangian equation is then solved using the algorithm of alternate direction multipliers [20].

The values of the number of components K and penalty  $\alpha$  play a significant role in VMD decomposition performance [21]. Specifically, a large value of K indicates interferential decomposition, whereas a small value indicates incomplete decomposition. As a result, the best values for K and  $\alpha$  must be determined. Therefore. The problem formulation is being reformulated as follows.

Assume  $y(t)$  represents a TEC time series. The goal of this study is to predict its value for the future time horizon,  $T_f$ . Because of its non-stationary aspect, first, it must be decomposed using the type VMD procedure before forecasting. The result of the decomposition is K modes that are expressed as follows:

$$\sum_{k=1}^K u_k(t) = \hat{y} \quad (3)$$

The decomposition's objective function is formulated to maximizes the correlation between intrinsic components  $Corr$  such as.

$$Corr = \frac{Cov(y(t), \hat{y}(t))}{\sigma(y(t))\sigma(\hat{y}(t))} \quad (4)$$

$$\left\{ \begin{array}{l} [K, \alpha]^* = \\ argmin(1 - Corr) = argmin\left(1 - \frac{Cov(y(t), \hat{y}(t))}{\sigma(y(t))\sigma(\hat{y}(t))}\right) \end{array} \right. \quad (5)$$

2) *Genetic algorithm*: A genetic algorithm (GA) is a stochastic searching algorithm with heuristic knowledge. It provides a way to find the optimal value of an objective function based on random generating of candidate solutions, heuristic interaction between them, and selecting elites from one generation to provide the offspring representing the next generation until convergence or meeting the stopping criterion [22]. GA is inspired by the theory of survival of the fittest that was proposed by Darwin [23]. The GA pseudocode is given in Algorithm 1.

Algorithm 1 GA Optimization

```

Input
    S //number of solutions in generation
    N//number of generations
    Objective function
Output
    Best solution
Start
    1- Initiate first population
    2- Current generation =first population
    3- Evaluate current generation
    4- Select elites (using roulette wheel)
    1- Perform crossover ((using uniform crossover) and mutation
    (using probability)
    2- Combine solutions
    3- if not meeting stopping criterion go to 3
    4- best solution =solution of best fitness value of the last
    generation
End
    
```

GA was employed to optimize the objective function of the decomposition Equation 5, and the two variables K and  $\alpha$  represent the chromosome. Algorithm 1 shows the steps of GA to obtain the best K and  $\alpha$  values. The first step consists of randomly generating the initial population in this work. The population is evaluated based on the objective function stated in Equation 5. Then, a roulette wheel selection mechanism is applied to select the parent that will undergo the crossover operation, used within a specific probability.

Similarly, the mutation operator is performed on the new solution within a pre-defined probability to maintain the diversity of the population. After that, the produced population will replace the worst solutions of the previous generation. These steps are repeated till meeting the stopping criterion. Finally, GA will return the best solution (i.e., best K and  $\alpha$  values).

3) *The Elman neural network*: An Artificial Neural Network, or ANN, is a massively parallel distributed processing system made up of densely interconnected neural computing parts that can learn, gain knowledge and make it available for use. ANN architecture is defined by the network of neuron connections, the training or learning mechanism for calculating the connection weights, and the activation function.

Even though the Multilayer Perceptron neural network (MLP) can solve a wide range of complex issues, it can only map the input space to the output space in a static way. Elman Neural Network (ENN) [24] is a simple recurrent neural network with dynamic characteristics. The structure of Elman RNN is identical to a three-layered MLP, except for an additional layer called a context layer, which is engaged in the former. In Elman RNN, the hidden neurons are activated by both the input and context neurons. The hidden neurons feed forward to activate the output neurons while also feeding back to activate the context neurons. As a result, the context layer allows ENN to respond to dynamism.

The ENN is trained using the BP algorithm, as shown in Equation 6 [25].

$$W(t + 1) = W(t) - \mu \frac{\partial E(t)}{\partial W(t)} \quad (6)$$

where,  $\mu$  denotes the learning rate.

A conceptual diagram of Elman RNN is presented in Fig. 1.

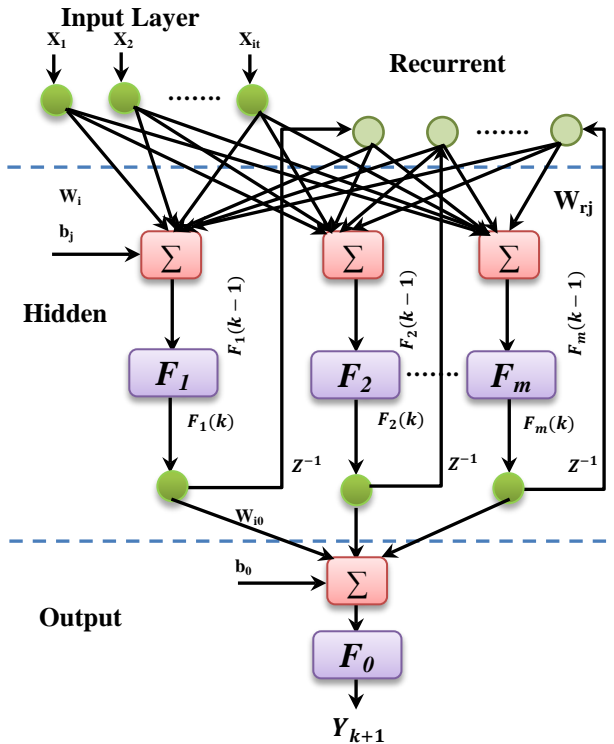


Fig. 1. The Structure of ENN [26].

**B. Methodology Flow**

As shown in Fig. 2, the developed methodology of the forecasting method consists of three phases after pre-processing: 1- Optimized VMD Decomposition, 2 - Elman RNN training, and 3 - forecasting. The phases are conceptual, but practically they have an interconnected nature. The optimization requires calculating the loss function to rank candidate solutions. On the other hand, the optimal evaluation setting is used for the VMD decomposition. Next, the result is used for ENN training and the trained ENN is used for forecasting.

1) *Phase 1: Optimized VMD Decomposition:* As is presented in Fig. 2, in the first phase, the data is entered into the optimized VMD decomposer, which is responsible for dividing the time series into various IMF components with the assistance of a genetic algorithm that optimizes K and  $\alpha$  values.

2) *Phase 2: ENN Training:* After decomposing the TEC time series into its IMF components in the first phase, the IMF passed to the recursive neural networks (ENN) to train the ENN model. The training phase comprises of two parts: the first part is the backward path that takes an existing neural network topology and calculates weight changes based on the gradient of the error. The second part is the forward path that uses current weights to propagate.

3) *Phase 3 Forecasting:* Once the ENN is trained, the testing phase (forecasting) is used. It uses the optimized VMD and trained ENN for forecasting the IMFs and after that a summation of the forecasted time series is used to forecast the overall time series. Such an evaluation includes providing the discrepancies between the predicted values and the actual values.

**C. Training and Testing Flow**

The interaction between the training phase and the testing phase is given in Fig. 3. As it is shown in the figure, the data comes as s stream, and it is partitioned into two parts: the historical part  $w_h$  and the future part  $w_f$ . The data in  $w_h$  was used for training, while the data in  $w_f$  was for performance evaluation. For the testing, the predicted value was compared with the original value stored in  $w_f$  and used to calculate testing errors.

**D. Data pre-processing and partitioning**

Pre-processing comprises data visualization and determining whether missing records exist. In the case of missing records, an average window over multiple days is used to replace the missing value in one day. After that, the data were partitioned. The purpose is to divide the data into training and testing data. The training data will come from the past, whereas the testing will occur in the future, forecasting time intervals. The signal and the duration of the time window are inputs. The output is a matrix consisting of training and testing data. The data will be passed through the time window, and samples will be added. The final sample is a prediction based on these samples. Following data collection, the data is divided into two categories: training and testing.

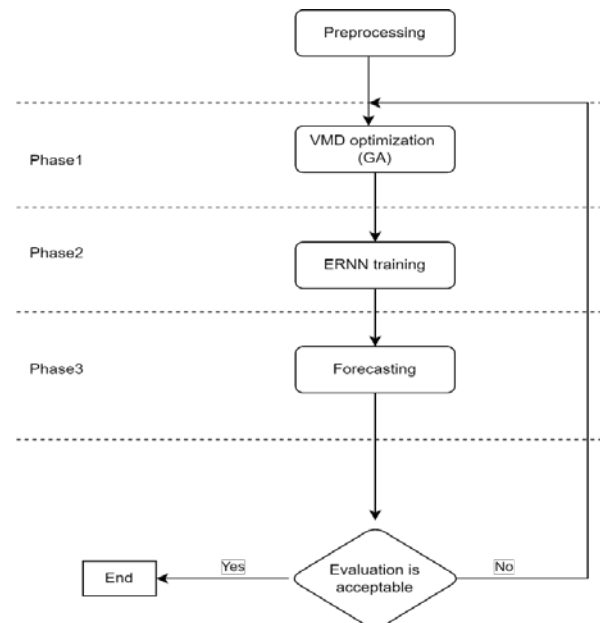


Fig. 2. A General Methodology Flowchart in TEC Forecasting.

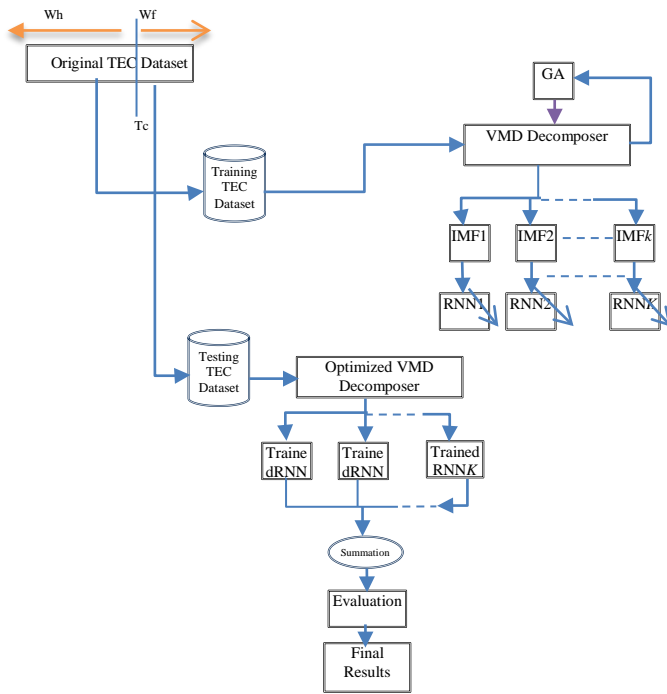


Fig. 3. Training and Testing Phases of TEC Forecasting.

E. Data Description

Data are recorded by the GPS Ionosphere Scintillation and TEC Monitor (GISTM) with a dual-frequency receiver GSV4004B at UKM station, geographic coordinate: 2.55 °N, 101.46 °E. At the L1 (1575.42 MHz) and L2 (1227.6 MHz) frequency bands, the GSV4004B receiver can track up to 11 GPS satellites. Amplitude and phase are monitored at 50 Hz, while code/carrier divergence (C/No) is sampled at 1 Hz for each satellite. The GPS Ionospheric Scintillation and TEC Monitor (GISTM) shows ionospheric delay over Universiti Kebangsaan Malaysia (UKM) station from 2011 to 2013.

F. Parameter Setting

GA optimization has been employed to find the best values of  $K$  and  $\alpha$ . Considering that the optimization process consumes considerable computational time, only a few numbers of individuals were permitted to participate. For GA, the number of iterations is set to 6, the number of individuals to 5, the searching range for  $K$  between 2 and 16, and the searching range for  $\alpha$  between 1,000 and 10,000 for GA optimization. The parameters are shown in Table I.

The proposed method has also been compared to ARIMA using the parameters mentioned in Table II. The observation's lag time is set to 30, the degree of difference is set to 2, and the moving window size is set to 15.

TABLE I. PARAMETER SETTING FOR GA

Dataset	No. of iterations	Crossover prob.	Mutation prob.	$K$	$\alpha$
2011-2012	6	0.5	0.3	[2,16]	[1000,10000]
2013	10	0.5	0.3	[2,16]	[1000,10000]

TABLE II. ARIMA PARAMETER SETTINGS

Parameter name	Value
Number of lag observations (p)	30
Degree of differencing (d)	2
Moving average window size	15

For ENN, the number of epochs was set to 6 and 10 for 2011 & 2012 and 2013, respectively. The number of neurons in the first layer was set to 60; the second layer was set to 30. The time window lag was set to 30. The parameter settings are shown in Table III.

TABLE III. ELMAN RNN PARAMETER SETTINGS

Parameter name	2011 & 2012	2013
Number of epochs	6	10
Neurons present in the First layer	50	50
Neurons in the hidden layer	30	25
Time-window (time lag)	30	30

G. Performance Metrics

The evaluation is based on two measures:

The first one is the mean squared error (MSE) which is given to evaluate the prediction of one time series, and is given by Equation 7.

$$MSE = \frac{1}{n} \sum_{t=1}^n (Y_t - F_t)^2 \tag{7}$$

where,  $Y_t$  denotes the ground truth value of the time series at moment  $t$ , and  $F_t$  denotes the predicted value of the time series.

The second metric is the improvement percentage from one model to another, and it is used to evaluate the relative improvement of proposed model over the benchmark as shown in Equation 8.

$$Percentage = \left| \frac{MSE_{Our} - MSE_{RMSE}}{MSE_{RMSE}} \right| \tag{8}$$

IV. EXPERIMENTAL RESULTS AND ANALYSIS

This section presents the obtained results from the experiments conducted in this study and analysis the results of the developed OVMD-RNN and its comparison with the benchmark ARIMA.

For the 2011 and 2012 datasets, 21 months were used for training and the remaining three months for testing. Fig. 4 depicts the original TEC time series for 2011 and 2012 before applying the proposed model, and the non-stationarity (the frequency varies over time) can be seen. Fig. 5 shows the testing data's TEC time series for three consecutive months.

For further evaluation, the proposed model has been tested on another dataset for the year 2013. Fig. 6 depicts the original TEC time series for 2013 before applying the proposed model. Fig. 7 is the TEC time series for two consecutive months for the testing data.

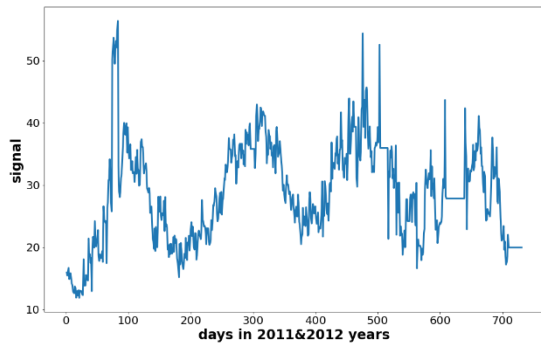


Fig. 4. TEC for 2011 and 2012 Dataset.

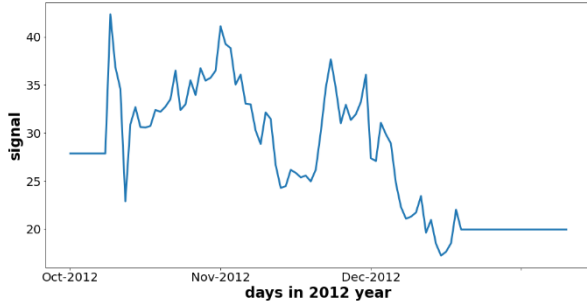


Fig. 5. TEC Time Series for Three Consecutive Months for Testing Data.

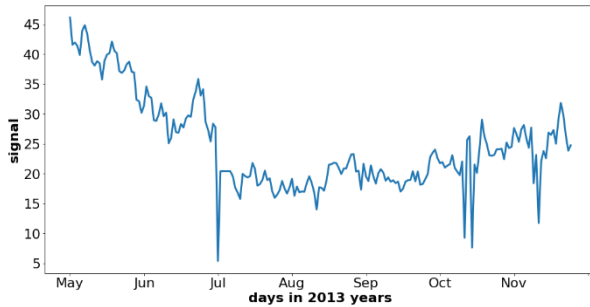


Fig. 6. TEC for 2013 Dataset.

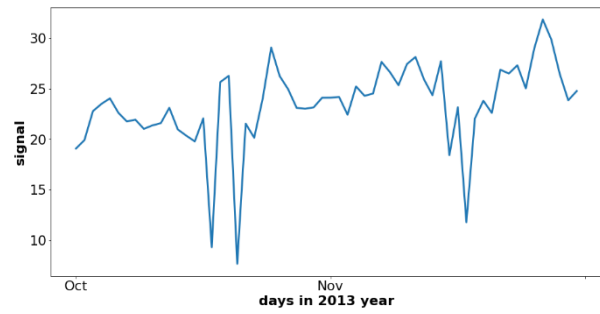


Fig. 7. TEC Time Series for Two Consecutive Months for Testing Data.

#### A. VMD Decomposition

1)  $K=5$ : Firstly, the TEC time series for 2011-2012 has been decomposed into its components using VMD and analyzed into five IMFs, which representing the optimal number of  $K$  components obtained through GA optimization, as shown in Table IV. Fig. 8 shows  $K=5$  components for the test TEC time series data part.

2)  $K=7$ : As shown in Fig. 9, the testing TEC time series for 2013 was decomposed into its components and analysed into seven IMFs representing the optimal number of  $K$  components obtained through GA optimization.

#### B. Forecasting

Fig. 10, for example, displayed the visualisation of mode 2 forecasting and their comparison to real values. The visualization of mode 4 forecasting and its comparison to real values are depicted in Fig. 11. The visualisation shows that the proposed model OVMD-RNN can follow all the up and down peaks in the original data.

TABLE IV. THE BEST  $K$  AND  $\alpha$  VALUE BY THE GA

Best $K$	Best $\alpha$	Algorithm
5	9948	GA

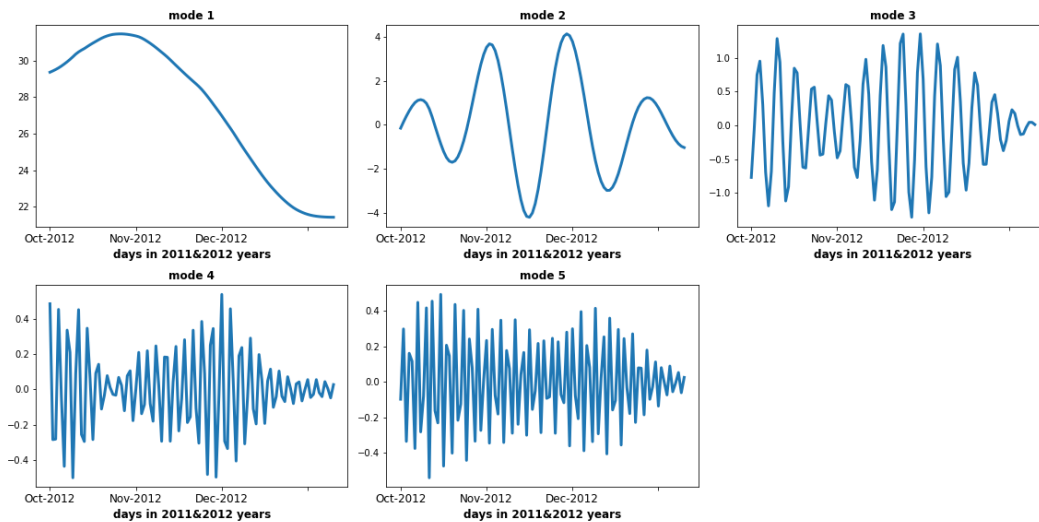


Fig. 8. VMD Decomposition for  $K=5$  for Testing Data.

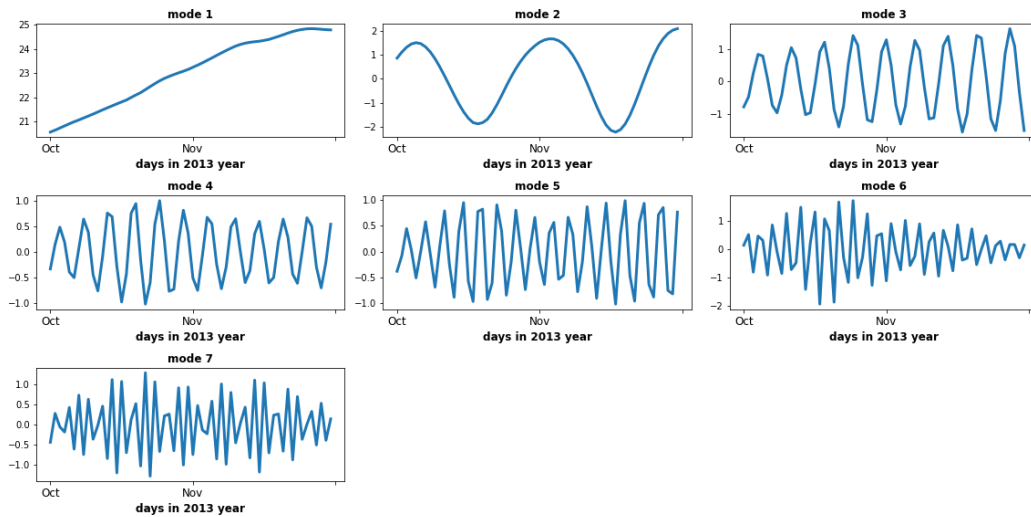


Fig. 9. VMD Decomposition for K=7 for Testing Data.

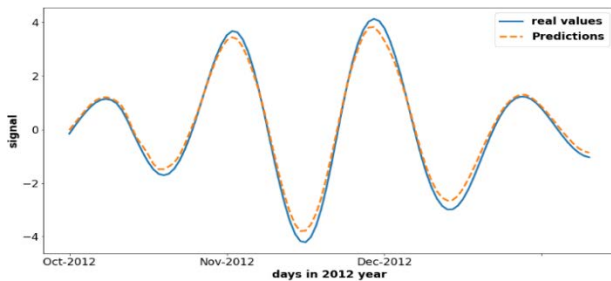


Fig. 10. Real Values Vs Prediction of VMD Mode 2.

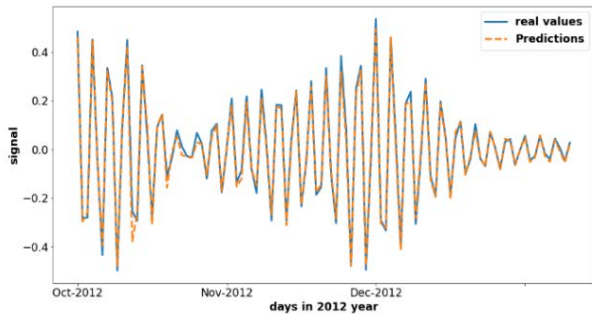


Fig. 11. Real Values Vs Prediction of VMD Mode 4.

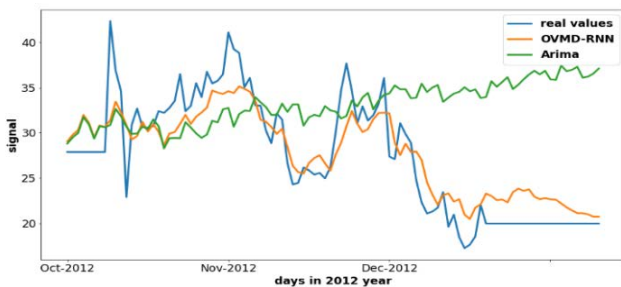


Fig. 12. A Comparison between Real Values, OVMD\_RNN and ARIMA for K = 5.

The forecasting results have been presented in Fig. 12. It is observed from the figure that in the three models, the

proposed model has provided better forecasting compared with ARIMA, which has shown a lack of capturing the trend and the pattern in the original time series. Furthermore, it has been discovered that the proposed model correctly predicted the four peaks in the original data, which show a level of 40 in October and November and a little lower level in late November and early December.

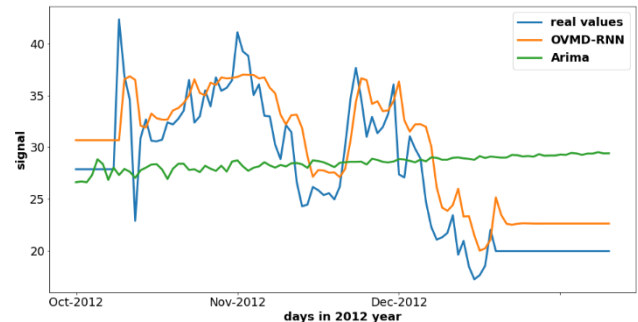


Fig. 13. A Comparison between Real Values, OVMD\_RNN and ARIMA for K = 1 (without VMD).

Fig. 13 presented the forecasting results for the years 2011&2012 in the last three months. Without applying VMD (K=1), observing Fig. 12, 13, it is noticed that K=1 has better tracking than a higher loss at the training. VMD interprets it has caused the removal of an essential part of the signal, which has led to missing by the neural network while training for K= 5, when K=1, this has not been observed because this part was preserved when training by ENN. This provides that VMD based training might not always provide good results due to the residual signal that is deleted by this process.

For further evaluation, the forecasting behavior in the year 2013 is presented for the proposed model and its comparison with ARIMA.

As is shown in Fig. 14 and 15 increasing the value of K has enabled better prediction. Furthermore, the model has successfully tracked all the up and down patterns in the time series, ranging between 15 and 30.

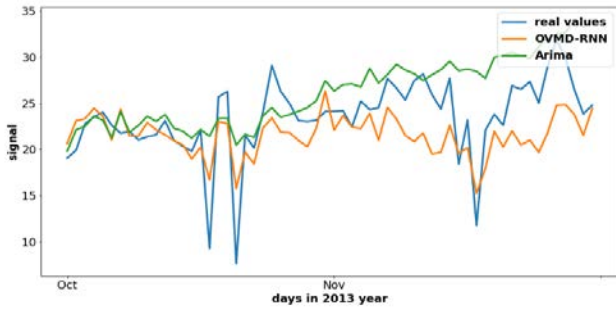


Fig. 14. A Comparison between Real Values, OVMD\_RNN and ARIMA for K = 7.

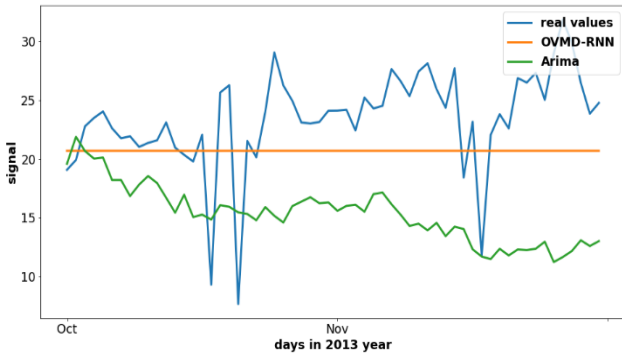


Fig. 15. A Comparison between 2013 Real Values, OVMD\_RNN and ARIMA for K = 1 (without VMD) and K = 7.

Fig. 14 presented the forecasting results for the year 2013 in the last two months because the first months have been used for training. It is observed from the figure that the proposed model has provided better forecasting compared with ARIMA, which has shown a lack of capturing the trend and the pattern in the original time series. In addition, it is noticed that the proposed model has successfully forecasted all the up and down peaks in the original data, which appears with the level of 10 for October and at the end of November with the level of 35.

Fig. 15 presented the forecasting results for the year 2013 in the last two months. Without applying VMD (K=1), the model can't track the trend of the time series.

### C. Evaluation

The evaluation was focused on creating the loss value and comparing it to the ARIMA benchmark.

1) *Loss value:* The loss value in the training phase is presented in Fig. 16, which shows that K=1 has the highest loss value than K=5, which is the value resulting from GA. In addition, for leading the optimality of GA.

Observing Fig. 13, it is noticed that K=1 has better tracking than a higher loss at the training. In K=5, the VMD process removed some important parts and caused some missing during Elman training. The result shows VMD-based training might not always provide good results due to the residual signal deleted by the process.

The loss value in the training phase is presented in Fig. 17 for the dataset 2011-2012, which proves the superiority of the proposed forecasting model when the value of K is selected optimally.

Regarding the loss value K=5, the proposed model has been compared to ARIMA, as shown in Fig. 17. The proposed approach has a smaller error or loss value than ARIMA. The results demonstrate that it is superior.

To summarize the performance, the overall loss value K=1 has been presented, which indicates VMD decomposition and K=7, which suggests the result of GA.

In Fig. 14 and 15, it is observed that increasing the value of K from 1 to 7 has enabled a lower value of loss than ARIMA, which proves the superiority of the proposed forecasting model when the value of K is selected optimally.

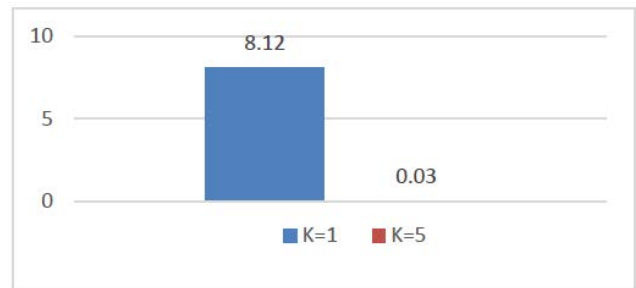


Fig. 16. The Loss Value of OVMD-RNN for When K =1, K=5.

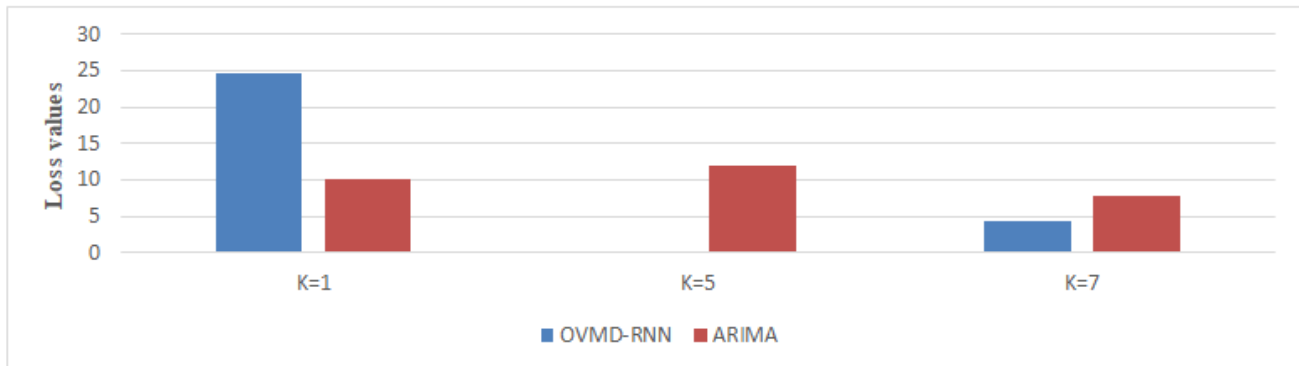


Fig. 17. The Loss Value of OVMD-RNN Vs ARIMA.



2) *Accuracy*: In terms of the loss value  $K = 5$ , OVMD-RNN has been compared to ARIMA, as shown in Fig. 12. Because proposed approach has a smaller error or loss value than ARIMA, the results demonstrate that it is superior. The improvement percentage is 99% as calculated based on Equation 9.

$$\text{Percentage} = \left| \frac{RNN-ARIMA}{ARIMA} \right| = \left| \frac{0.05-12.47}{12.47} \right| = 0.99 \quad (1)$$

TABLE V. OVERALL PREDICTION COST FOR ARIMA AND OVMD-RNN BASED ON DIFFERENT YEARS AND VALUES OF K

K	2011&2012		2013	
	1	5	1	7
ARIMA	6.92	12.04	10.14	7.79
OVMD-RNN	8.12	0.03	24.72	4.29
Improvement percentage	0.17	99%	%143	%44

From Table V,  $K = 1$  indicates that VMD has not been applied. So, the non-stationary time series were not divided into stationary components but were predicted directly using ENN and ARIMA. For  $K = 5$  and  $K = 7$ , these values were obtained by implementing GA on both times series 2011-2012 and 2013, respectively, to find the best K value. These K values provide the lowest loss value.

#### D. Observations

From the results obtained, it has been observed that TEC is a non-stationary time series making it challenging to forecast. Moreover, VMD is a good candidate for decomposing TEC time series into stationary components. Still, sometimes VMD-based training might not always provide good results due to the residual signal.

The proposed model (OVMD-RNN) does not implement multi-time series collected from different areas to be generalized. Therefore, extending the model to accept multi-time series at one time will enable more accurate forecasting; this can be applied for future work.

### V. SUMMARY AND CONCLUSION

This paper has created a novel forecasting approach for the TEC time series. VMD is used to split the original TEC time series into necessary stationary components, considering the non-stationarity of the data and the need to include non-linear knowledge for forecasting. Each essential TEC component was trained and forecasted using an Elman RNN. In addition, the method consists of an optimization algorithm for determining the best VMD decomposer parameters. The VMD parameters, K and  $\alpha$  selection, utilized the GA optimization method. The GPS Ionospheric Scintillation and TEC Monitor (GISTM) with a dual-frequency receiver GSV4004B at the UKM station evaluated our obtained dataset for three years, 2011, 2012 and 2013. The evaluation was focused on creating the loss value and comparing it to the ARIMA benchmark. It showed that the proposed progressive technique with two decomposition values for  $K = 4$  and 5 and a significant reduction of the loss value was superior. Future research will develop multi-dimensional TEC forecasting from multiple places within the same geographic region.

### ACKNOWLEDGMENT

We like to thank the Data Mining and Optimization (DMO) Lab of Faculty of Information Science and Technology, Universiti Kebangsaan Malaysia (UKM), College of Science for Women, University of Babylon, Iraq for the expert's knowledge sharing, and the Space Science Centre (ANGKASA) UKM, for providing the data. Massive appreciation to UKM for providing grant GGP-2020-032 for funding this research and the Iraq Government for sponsoring the postgraduate study.

### REFERENCES

- [1] L. Mallika, D. V. Ratnam, S. Raman, and G. Sivavaraprasad, "Machine learning algorithm to forecast ionospheric time delays using Global Navigation satellite system observations," *Acta Astronautica*, vol. 173, pp. 221-231, 2020.
- [2] U. Sezen, T. L. Gulyaeva, and F. Arikan, "Online international reference ionosphere extended to plasmasphere (IRI-Plas) model," in 2017 XXXIIInd General Assembly and Scientific Symposium of the International Union of Radio Science (URSI GASS), 2017, pp. 1-4: IEEE.
- [3] A. A. Akyol, O. Arikan, and F. Arikan, "A machine learning-based detection of earthquake precursors using ionospheric data," *Radio Science*, vol. 55, no. 11, pp. 1-21, 2020.
- [4] D. V. Ratnam, Y. Otsuka, G. Sivavaraprasad, and J. K. J. A. i. S. R. Dabbakuti, "Development of multivariate ionospheric TEC forecasting algorithm using linear time series model and ARMA over low-latitude GNSS station," vol. 63, no. 9, pp. 2848-2856, 2019.
- [5] M. Kaselimi, A. Voulodimos, N. Doulamis, A. Doulamis, and D. J. R. S. Delikaraoglou, "A Causal Long Short-Term Memory Sequence to Sequence Model for TEC Prediction Using GNSS Observations," vol. 12, no. 9, p. 1354, 2020.
- [6] S. Inyurt, M. Hasanpour Kashani, and A. Sekertekin, "Ionospheric TEC forecasting using Gaussian Process Regression (GPR) and Multiple Linear Regression (MLR) in Turkey," *Astrophysics and Space Science*, vol. 365, no. 6, p. 99, 2020/06/10 2020.
- [7] K. Ansari, S. K. Panda, O. F. Althwaynee, and O. Corumluoglu, "Ionospheric TEC from the Turkish Permanent GNSS Network (TPGN) and comparison with ARMA and IRI models," *Astrophysics Space Science*, vol. 362, no. 9, pp. 1-14, 2017.
- [8] S. Salma, G. Sivavaraprasad, B. Madhav, and D. V. Ratnam, "Implementation of VARMA Model for Ionospheric TEC Forecast over an Indian GNSS Station," in 2020 5th International Conference on Devices, Circuits and Systems (ICDCS), 2020, pp. 144-148: IEEE.
- [9] L. R. Cander, "Ionospheric space weather forecasting and modelling," in *Ionospheric space weather*: Springer, 2019, pp. 135-178.
- [10] J. B. Habarulema, L.-A. McKinnell, and P. J. Cilliers, "Prediction of global positioning system total electron content using neural networks over South Africa," *Journal of Atmospheric solar-terrestrial physics* vol. 69, no. 15, pp. 1842-1850, 2007.
- [11] J. B. Habarulema, L.-A. McKinnell, P. J. Cilliers, and B. D. Opperman, "Application of neural networks to South African GPS TEC modelling," *Advances in Space Research*, vol. 43, no. 11, pp. 1711-1720, 2009.
- [12] G. Sivavaraprasad and D. V. Ratnam, "Performance evaluation of ionospheric time delay forecasting models using GPS observations at a low-latitude station," *Advances in Space Research*, vol. 60, no. 2, pp. 475-490, 2017.
- [13] N. Elmumim, M. Abdullah, A. Hasbi, and S. Bahari, "Comparison of GPS TEC variations with Holt-Winter method and IRI-2012 over Langkawi, Malaysia," *Advances in Space Research*, vol. 60, no. 2, pp. 276-285, 2017.
- [14] G. Sivavaraprasad, D. V. Ratnam, M. Sridhar, and K. Sivakrishna, "Modelling and forecasting of ionospheric TEC irregularities over a low latitude GNSS station," *Astrophysics Space Science*, vol. 365, no. 10, pp. 1-14, 2020.

- [15] Z. Huang, Q. Li, and H. Yuan, "Forecasting of ionospheric vertical TEC 1-h ahead using a genetic algorithm and neural network," *Advances in Space Research*, vol. 55, no. 7, pp. 1775-1783, 2015.
- [16] M. R. G. Razin and B. Voosoghi, "Modeling of ionosphere time series using wavelet neural networks (case study: NW of Iran)," *Advances in Space Research*, vol. 58, no. 1, pp. 74-83, 2016.
- [17] J. R. K. K. Dabbakuti, A. Jacob, V. R. Veeravalli, and R. K. Kallakunta, "Implementation of IoT analytics ionospheric forecasting system based on machine learning and ThingSpeak," *IET Radar, Sonar Navigation*, vol. 14, no. 2, pp. 341-347, 2019.
- [18] G. Li, X. Ma, and H. Yang, "A hybrid model for monthly precipitation time series forecasting based on variational mode decomposition with extreme learning machine," *Information*, vol. 9, no. 7, p. 177, 2018.
- [19] R. Jegadeeshwaran, V. Sugumaran, and K. Soman, "Vibration based fault diagnosis of a hydraulic brake system using Variational Mode Decomposition (VMD)," *Structural Durability Health Monitoring*, vol. 10, no. 1, p. 81, 2014.
- [20] C. Zhao et al., "Novel method based on variational mode decomposition and a random discriminative projection extreme learning machine for multiple power quality disturbance recognition," *IEEE Transactions on Industrial Informatics*, vol. 15, no. 5, pp. 2915-2926, 2018.
- [21] M. Niu, Y. Hu, S. Sun, and Y. Liu, "A novel hybrid decomposition-ensemble model based on VMD and HGWO for container throughput forecasting," *Applied Mathematical Modelling*, vol. 57, pp. 163-178, 2018/05/01/ 2018.
- [22] M. A. A. Albadr, S. Tiun, M. Ayob, F. T. Al-Dhief, K. Omar, and F. A. Hamzah, "Optimised genetic algorithm-extreme learning machine approach for automatic COVID-19 detection," *PLoS one*, vol. 15, no. 12, p. e0242899, 2020.
- [23] Mirjalili, S., Song Dong, J., Sadiq, A.S. & Faris, H. 2020. Genetic algorithm: Theory, literature review, and application in image reconstruction. *Nature-Inspired Optimizers* 69–85.
- [24] Kamanditya, B. & Kusumoputro, B. 2020. Elman recurrent neural networks based direct inverse control for quadrotor attitude and altitude control. In *2020 International Conference on Intelligent Engineering and Management (ICIEM)*. pp. 39–43. IEEE.
- [25] G. Ren, Y. Cao, S. Wen, T. Huang, and Z. Zeng, "A modified Elman neural network with a new learning rate scheme," *Neurocomputing*, vol. 286, pp. 11-18, 2018.
- [26] R. Hannah Jessie Rani and T. Aruldoss Albert Victoire, "A hybrid Elman recurrent neural network, group search optimization, and refined VMD-based framework for multi-step ahead electricity price forecasting," *Soft Computing*, vol. 23, no. 18, pp. 8413-8434, 2019.